IEEE Access
Multidisciplinary | Rapid Review | Open Access Journal

Received October 3, 2021, accepted October 29, 2021, date of publication November 8, 2021, date of current version November 11, 2021.

Digital Object Identifier 10.1109/ACCESS.2021.3125710

Propagation Measurement of a Pedestrian Tunnel at 24 GHz for 5G Communications

QI PING SOO[1], (Member, IEEE), SOO YONG LIM[1], (Senior Member, IEEE), NURHIDAYAH RUSLI[1], KA HENG CHONG[1], DAVID WEE GIN LIM[1], (Senior Member, IEEE), HENG-SIONG LIM[2], (Senior Member, IEEE), ZHENGQING YUN[3], (Senior Member, IEEE), AND MAGDY F. ISKANDER[3], (Life Fellow, IEEE)

[1]Department of Electrical and Electronic Engineering, University of Nottingham Malaysia, Semenyih 43500, Malaysia
[2]Faculty of Engineering and Technology, Multimedia University, Bukit Beruang, Melaka 75450, Malaysia
[3]College of Engineering, Hawai'i Advanced Wireless Technologies (HAWT) Institute, University of Hawaii at Manoa, Honolulu, HI 96822, USA

Corresponding author: Soo Yong Lim (Grace.Lim@nottingham.edu.my)

This work was supported in part by the Fulbright-Malaysian Communications and Multimedia Commission (MCMC) U.S. Specialist Program under Grant FSP-P002144.

ABSTRACT In this paper, we report the results of a field measurement campaign carried out inside a pedestrian tunnel at 24 GHz in two conditions, namely, empty tunnel scenario and busy tunnel scenario with pedestrian movement. The experiment measures the fading effects of various groups of pedestrian crowds using directional antennas at the transmitter and receiver for millimeter-wave radio communications. Having presented and analyzed the measurement data in several diverse scenarios, we have further investigated human scattering effects in the crowded pedestrian tunnel and performed ray-tracing simulation for an empty pedestrian tunnel condition. Because tunnel is an enveloped scenario that is not bound by any geographic areas, the results of this study can be applied to a wider scenario like other pedestrian tunnels across the globe. Above all, these findings contribute towards ensuring wireless connectivity for everyone even in a remote scenario like underground passages.

INDEX TERMS 5G communications, radio propagation, propagation measurement, ray-tracing.

I. INTRODUCTION

In a modern society, people are constantly on the move – in the air, on the ground, across the ocean, through the underground passageway, and on foot. While commuting from one place to another, they are constantly connected on various gadgets, especially the younger generations and even through remote passageway like tunnel. This is a totally different scenario from the olden days' tunnel/coal mining condition where communication inside those structure was unavailable or near impossible – until the study in 1975 to attempt investigating the propagation environment of coal mines in addressing their communication needs therein [1]. Since then, the usage of tunnels has extended from its original use in the coal mining industry to account for other aspects such as energy, water and telecommunication needs. To that end sewerage, water, electrical and communication cable, as well as flood storage tunnels are built. Nevertheless, despite the wide use of tunnels in a great variety of domains, the primary use of tunnels remains for transportation, anything ranging from road to railway, and from mass transit to pedestrian use. With the advancement of technology, increasingly more people worldwide commute daily by underground traffic infrastructures such as underground passages, walkways, and tunnels. Because of this mushrooming phenomenon, mobile operators are faced with a real challenge to provide reliable services in underground environments and yet maintain the same quality standard as that of above-ground scenarios to the end users [2].

The novelty of our work is such. Current propagation models developed for tunnels deal almost all with vehicles traffic [3]–[5], and this differs from pedestrian traffic in indoor tunnel/passages scenarios. Therefore, the existing propagation models cannot be directly applied to indoor tunnel and underground passages environments to obtain accurate propagation prediction results. Also, literature survey shows that crowd effects are significant at the millimeter wave, but little is known about how crowd is affecting the pedestrian tunnel environment to date. Hence our work aims to close this gap by investigating how crowd is affecting the pedestrian tunnel environment by conducting field measurement while taking into account the beamforming effects at the millimeter

The associate editor coordinating the review of this manuscript and approving it for publication was Hussein Attia.

wave (mm-wave). It is for this purpose that we undertook a joint venture among three parties to explore the propagation environment of one of the world's busiest pedestrian tunnels in the heart of Kuala Lumpur (KL) at 24 GHz – an unlicensed band in Malaysia.

To date, even though numerous studies have been conducted on the topic of mm-wave, anything ranging from antennas design to microwave device development, the specific topic of the propagation of mm-wave in tunnels is still insubstantial. To trace back, the earliest study on tunnel propagation at the mm-wave band was reported in 1994 [6] as the focus of propagation in tunnels back in the late 20th century and the early 21th century has always been at the Ultra High Frequency (UHF) and Super High Frequency (SHF) bands. Nevertheless, in the recent five years, we observe that there is an increasing number of propagation studies reported at the mm-wave band for tunnels which can be broadly categorized into two categories, namely, low mm-wave band (25-30 GHz) [7]–[11], and high mm-wave band (60 GHz, 75 GHz) [4], [12]–[14]. While the scientific community recognizes the significant effects of the human bodies at the mm-wave, the specific topic of human bodies effects inside the pedestrian tunnel at the mm-wave has not been studied. Hence we have tailored made our measurement setup for this purpose while taking into consideration the beamforming effects. This makes our measurement setup unique as it adds value to the RF community by generating new knowledge on channel characteristics inside pedestrian tunnel whereby frequent and random people movement are rampant.

In Malaysia, 24 GHz is an unlicensed band. Millimeter waves promise to alleviate frequency congestion, thereby bringing a greater user satisfaction for a smoother and seamless connectivity. In the past, previous researchers have looked at several topics at the mm-wave network, such as vehicle obstruction and user self-obstruction [15], as well as vegetation effects [16]. On the specific topic of human activities at the mm-wave band, some researchers have investigated human bodies and their scattering/blockage effects [17]–[19]. Specifically, in [19], the effects of human bodies were studied in an enclosed room, and this may be of interest to our present study. And yet, their result is restricted to an enclosed room and cannot be applied directly to a long pedestrian tunnel.

The tunneling industry in Malaysia has made significant progress and major tunnels were constructed for various applications over the last one and a half decades. Chief among those tunnels is the realization of the Stormwater Management & Road Tunnel (SMART) tunnel to solve the problem of traffic congestion and flash flood dilemma in Kuala Lumpur [20]. In the early days, tunnels in Malaysia were associated mainly with railway such as the Butterworth-Singapore Line as well as with the gold and tin mining industries [21]. However, what chiefly drives the tunneling industry in Malaysia in recent years is the huge demands of transportation, aside from energy and water infrastructure projects. Take the SMART tunnel for example; this 9.7 km long tunnel is the longest storm water tunnel in Southeast Asia and the second longest in Asia. It is listed by the Cable News Network (CNN) as one of the top 10 world's greatest tunnels where the tunnel is foreseen to avoid billions of dollars in possible flood damage and costs from traffic congestion in KL city center [22], [23].

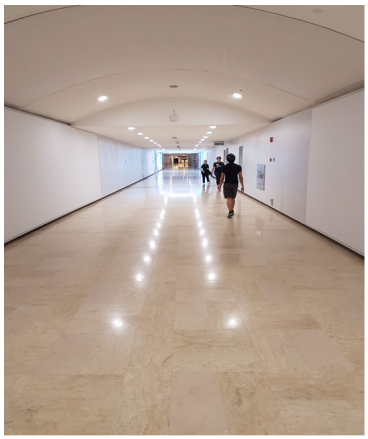

FIGURE 1. Picture showing the pedestrian tunnel linking between Suria KLCC and KL convention centre.

The chief problem being addressed by this manuscript is an investigation into the pedestrian effects on radio waves propagation inside one pedestrian tunnel at 24 GHz. This pedestrian tunnel is located between Suria KLCC (a shopping mall in Kuala Lumpur City Centre) and KL Convention Centre, linking the two buildings, see Fig. 1.

II. MEASUREMENT SET-UP

Measurement is a proven successful way to study a specific propagation environment. By conducting an actual field measurement, all the contributing rays to that particular environment are captured, and hence, path loss/gain can be subsequently analyzed. We have conducted field measurements to study several diverse propagation environments in the past, such as indoor stairwell [24], periodic building façade [25], open-trench drain [26], and more recently, natural cave [27]. Previous measurement works were conducted at the conventional frequency bands such as 900 MHz, 2.4 and 5.8 GHz. In this work, we have switched our focus for the first time to conduct field measurement at the mm-wave inside a pedestrian tunnel, which is among one of the busiest pedestrian tunnels in the world. The selected frequency is 24 GHz – this provide generous bandwidth and their use of much smaller antennas play a significant role in 5G network. Figs. 2 and 3 show the transmitter and receiver set-up.

As can be seen in Figs. 2 and 3, directional horn antennas are utilized in the assembly of the measurement unit. The horn antenna has 20 dB gain and half-power beam width of about 15 degree. On the transmitter (Tx) end, Anritsu MG3694C signal generator is employed, which can transmit signal up to 40 GHz. On the receiving end (Rx), Anritsu MS2830A spectrum analyzer is used, which functions in the range of 9 kHz to 43 GHz. Both the Tx and

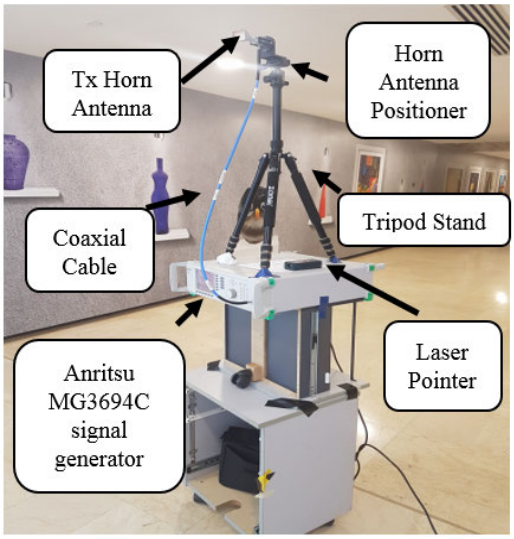

FIGURE 2. The set-up of the transmitter.

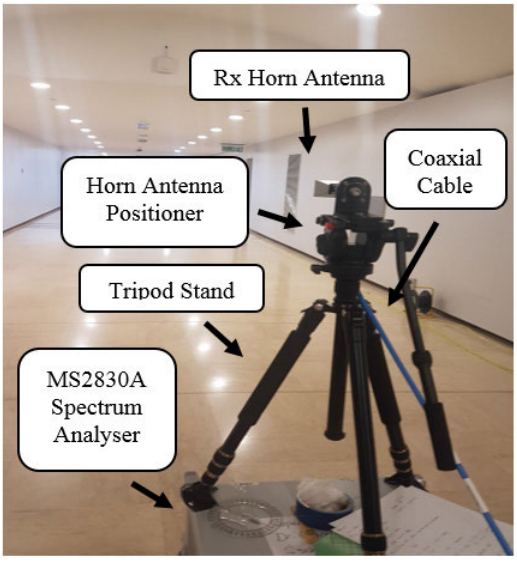

FIGURE 3. A close-up look of the receiver.

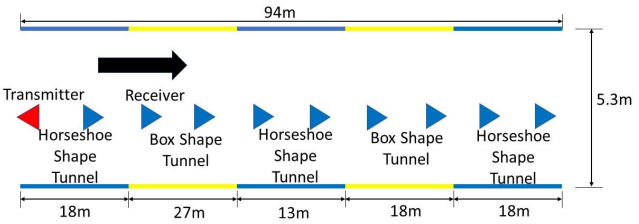

FIGURE 4. Geometry of the measurement route. (Top view.)

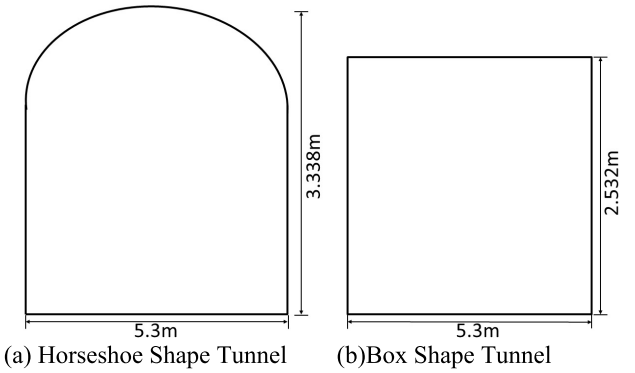

FIGURE 5. Geometry of the measurement route (front view).

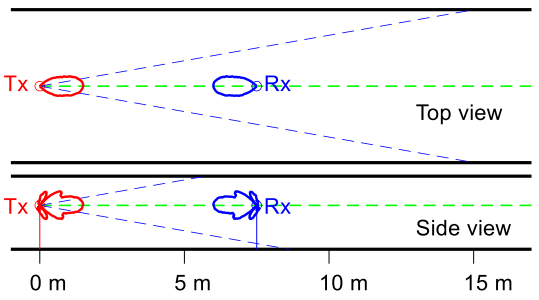

FIGURE 6. Geometry of the measurement route (first 15 meters) with real radiation pattern from the horn antennas. (Gain = 18.54 dB, 3dB Beamwidth (deg) at H-Plane = 20.20 and 3dB Beamwidth (deg) at E-Plane = 18.66.)

Rx horn antennas were placed directly facing towards each other during the measurement. As for the measurement data, it is acquired by the spectrum analyzer and subsequently deposited onto a computer for post-processing of data on MATLAB.

In addition to the pictures of the Tx and Rx, the geometry of the measurement route is provided in Fig. 4. It can be seen from Figs. 1 and 5 that the ceiling of the KLCC pedestrian tunnel is not entirely flat; rather, it is made up of two consecutive portions which we term as "horseshoe shape" and "box shape" sections. In the former, the "horseshoe shape" portion, the ceiling is of an arch-shape; whereas in the latter, the "box shape" portion, the ceiling is completely flat. These two different shape sections intersect each other consecutively. The height of the "horseshoe shape" ceiling is 3.338 m, while the height of the "box shape" ceiling is 2.532 m. The diameter of the tunnel is 5.3 m and the sides of the tunnel walls are made up of dry wooden board. Based on this dimension we can expect the tunnel to exhibit a certain degree of waveguiding effects, similar to that of a waveguide cross section of 5.3 m $\times$ 2.532 m. Beyond this, we can further foresee that numerous modes are excited to give a very good waveguiding effects in this tunnel.

Supplementary to Fig. 4, in Fig. 6, we visually display that most of the areas along the measurement route are covered by the main beam, and that most of the modes can be excited by the horn antennas. However, as the transmitter-to-receiver distance increases, the number of modes contributing to the overall received field decreases since the attenuation constant of the mode increases with the mode order.

III. PEDESTRIAN TUNNEL MEASUREMENT AT 24 GHz

The primary goal of conducting a field measurement campaign inside the KLCC pedestrian tunnel is to observe pedestrians' effects on the propagation of radio waves. To achieve this goal, we have strategized to conduct our experiments in two conditions, namely, an empty tunnel scenario, and a busy tunnel scenario. The KLCC pedestrian tunnel is open to the public from 7 a.m. to 11 p.m. daily. Therefore, it is not difficult to conduct our experiment for an empty tunnel scenario by simply selecting a time outside of the tunnel opening hours. In this scenario, for empty tunnel measurement, we have collected our experimental data in the early morning, between 5 am to 7am, before the tunnel was open to the public.

In our field measurement campaigns, two styles of data collection were employed. The first style is, during the measurement, the Tx antenna was placed at 1 m away from the first position of the Rx antenna. The Rx antenna, mounted on a roller cart, was pushed at a constant speed along the measurement route of a fixed distance, e.g. 50 m, 94 m. The second style is, Tx and Rx were placed at a fixed distance over a route of 20 m, 50 m, and 90 m, and the received signal strengths were recorded over a duration of 3 minutes. The main objective of using the second style of measurement is to observe human effects on signals inside the pedestrian tunnel at the mm-waves. In all cases, both the Tx and Rx antenna heights are 1.52 m for vertical-vertical (VV) polarization. Fig. 7 shows our tunnel measurement results inside an empty tunnel, where the experiment was conducted twice using the first style, and the results bear a strong resemblance to each other, proving its repeatability.

Aside from Fig. 7, to give an example of the second style of our data collection technique, Fig. 8 is plotted. This result was collected from the second round of measurement campaign during peak hours, i.e. 10 a.m. to 12 p.m. where pedestrian movement peaked in the tunnel. In Fig. 8, the Tx and Rx antennas heights are set to be 1.52 m, oriented for VV polarization over a fixed route of 20 m, 50 m, and 90 m. Both the Tx and Rx are static, hence, only pedestrian effects are observed. There were occasional deep fades of the signals, see for instance, those that occurred at approximately 1 minute and 2 minute of the sweep time, and these are due to human crossing the LoS path. We note that the change in the received power due to blocking is dramatic but it is masked by the fading effects due to crowd and becomes less obvious.

To compare the results of an empty tunnel with that of a busy tunnel, Fig. 9 is plotted. Based on visual observation, random number of pedestrians walked past our measurement routes at any one time. These people may not walk across to block the LoS path but they may be walking adjacent to the LoS path, in a random manner. Signals power are not always attenuated when people walk in parallel to the LoS path, sometimes they are enhanced. Fig. 9 is a typical set of result collected from several rounds of experiments, and it can be seen from this figure that the signal variation of the empty tunnel scenario is much less drastic than the busy tunnel scenario with pedestrian movement. Both Figs. 8 and 9 imply that pedestrian movement at the mm-waves such as 24 GHz has a significant impact on the received signal strength. The standard deviation at the three different fixed distances, i.e. 20 m, 50 m, and 90 m are computed as 0.14 dB, 0.37 dB, and 0.44 dB respectively, and these values can be used as fading margin for network planning considering the crowd effects.

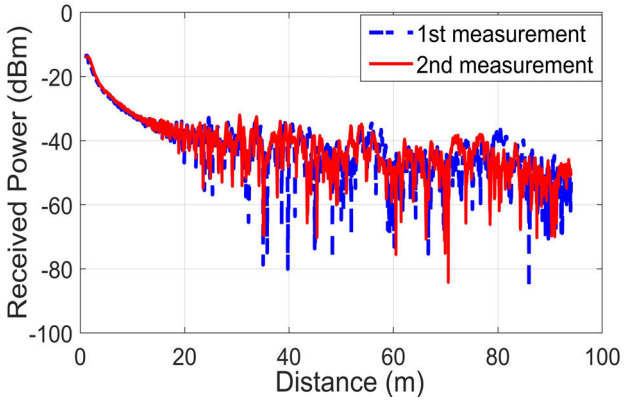

FIGURE 7. Repetition test for an empty pedestrian tunnel scenario.

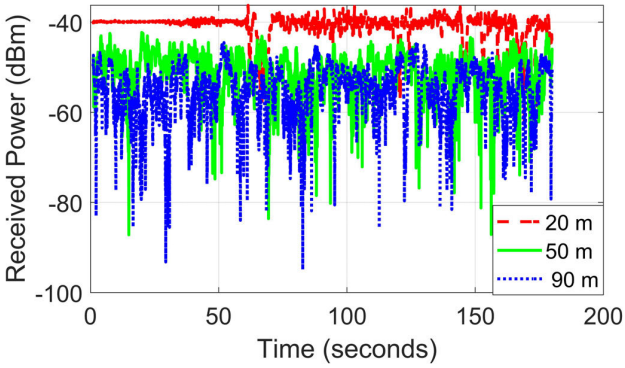

FIGURE 8. Typical collected signals from the second measurement style, whereby pedestrian effects are seen.

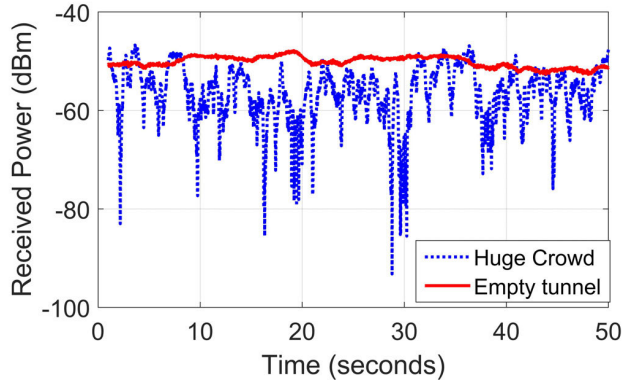

FIGURE 9. Comparison results between an empty and a crowded pedestrian tunnel over a fixed distance of 90 m in 50 seconds sweep time.

TABLE 1. Mean and standard deviation values of the averaging results.

Windows	Mean Values	Standard Deviation Values
20-wavelength	4.3834	7.4855
30-wavelength	4.3835	7.3723
40-wavelength	4.3836	7.2978

There was another variation that we have attempted, that was to raise the Tx to 1.926 m but kept the Rx at 1.52 m, and yet moved the Tx from the center to the right-hand side of the pedestrian tunnel. The Rx continued to move along the same measurement route right at the center of the pedestrian tunnel. Altering the set up gives us an additional perspective into the propagation environment of the pedestrian tunnel, since now we can investigate the placement position of the Tx and examine how that affects signal propagation in the same environment. The comparison results from this additional measurement are plotted in Fig. 10 where sharp differences are recorded only in the beginning of the measurement route, e.g. in the first 15 m or so.

The effect observed in Fig. 10 is due largely to the directional antennas we used in the measurement. When the Tx is moved to the right, the Rx is outside of the beam coverage for the first 15 m or so, which explains why the recorded signal strengths between the two graphs are very different in this portion. In other words, when the Rx moves nearer to the Tx in this region, it falls out from the main beam of the Tx. Yet when the separation distance between the Tx and Rx increases, especially after exceeding a certain threshold, it made no difference where the Tx antenna is positioned, whether to the far left, far right, or right at the center.

In an effort to get rid of the pedestrian effects to compare the mean signals with those in the empty tunnel, we have averaged the mean instantaneous signal over a 20-, 30-, and 40- wavelength windows based on the data in Fig. 10 (blue line, Tx at central). This averaging process has flattened the curve to get rid of the pedestrian (small scale fading) effects. Table 1 summarizes the mean values and the standard deviation values of the three averaging results.

From Table 1, we note that though the mean value remains about the same each time the averaging is performed on the measurement data, the standard deviation value drops when the wavelength window value increases. These two values are approximately 4.3 dB and 7.3 dB respectively. It's worth mentioning that the averaging process is done only on the crowded tunnel scenario but not for the empty tunnel scenario. For the empty tunnel scenario, we have presented the raw data as it is.

IV. FURTHER INVESTIGATION OF HUMAN SCATTERING EFFECTS AND EMPTY TUNNEL RAY-TRACING SIMULATION

In this section, we have further investigated human scattering effects in the crowded pedestrian tunnel and performed ray-tracing simulation for an empty pedestrian tunnel condition. First, for investigating human scattering effects in the crowded pedestrian tunnel, we have built a simple model to incorporate the effects of scattering off humans' head in a random manner. Fig. 11 displays how the scattering effect is considered off a human's head.

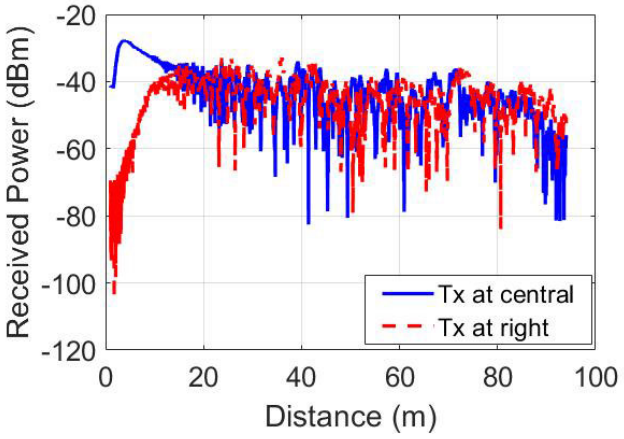

FIGURE 10. Measurement results showing the difference between two different positions of the Tx with a height of 1.926 m.

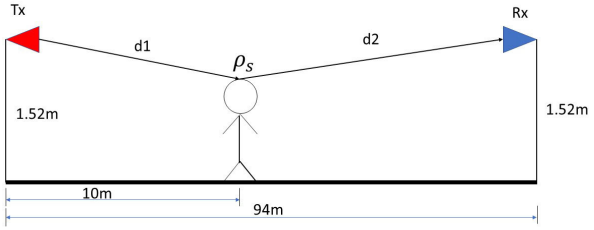

FIGURE 11. Scattering effects are considered off a human's head in the pedestrian tunnel.

As illustrated in Fig. 11, Tx sends out a ray that gets scattered off a human's head before reaching the receiver. The total distance travelled by the ray from the Tx to the Rx is the summation of distance 1 (d1) and distance 2 (d2). At the location where scattering takes place, we have included a scattering factor [28] to equation (1). Further details of the general ray-tracing technique are recorded in [29]. It is with this ray-tracing technique that subsequent simulations are performed for validation.

$$E_r = \frac{1}{r} e^{-j\beta r} \left(\frac{\lambda}{4\pi} \right) \rho_s \tag{1}$$

Equation (1) is the mathematical expression of the reflected ray off a human's head, where r is the distance along the reflected ray path, λ is the wavelength, β is the wave number, $e^{-j\beta r}$ is the phase factor, $\frac{\lambda}{4\pi}$ is a parameter related to the antenna effect, and ρ_s is the scattering factor. The scattering factor values are taken randomly from between -1 to $+1$ on MATLAB; and the size of the random data are defined by the number of people. The simulated people are randomly placed over the entire route of 94 m. Fig. 12 gives a glimpse of what happened when the number of people increases and as the Rx moves gradually away from the Tx; and Fig. 13 shows

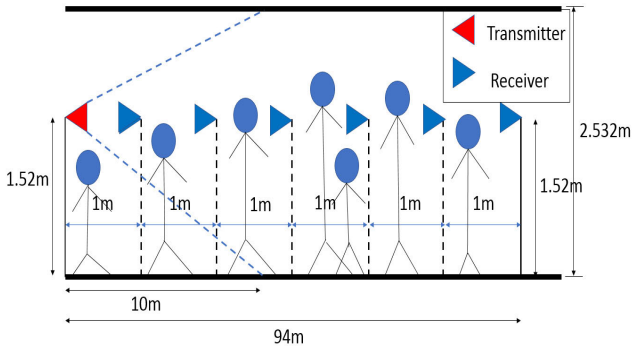

FIGURE 12. Illustration of more human heads are considered as the receiver moves gradually away from the transmitter.

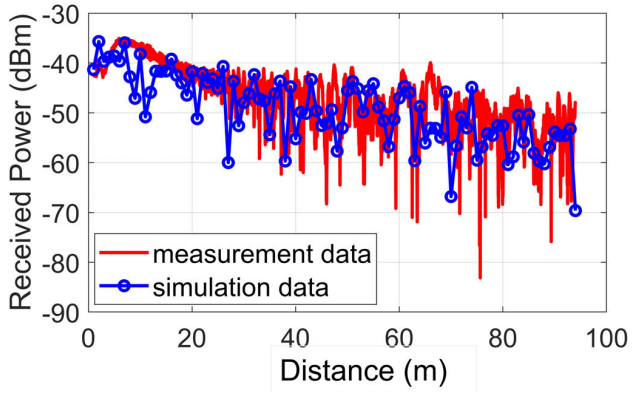

FIGURE 13. Humans scattering effects of between 20 to 30 people are compared with the measurement data.

how these human movement affects the propagation results. This figure is plotted to consider the surrounding wall effects and the scattering off humans' heads. The measurement data is taken from Fig. 10 (blue line, Tx at central), and this is a distance-varying result obtained from a crowded tunnel environment.

As illustrated in Fig. 12, the heights of the people are determined in a random manner to portray the real scenario as in real life where people of varying heights walk across the pedestrian tunnel. Initially, we have considered one human effect and gradually increased this number and stopped at 25, based on our estimation of the number of people that walked pass the measurement route during data collection. Fig. 13 shows the simulation results of between 20 to 30 people compared against the measurement data, where a good match is obtained. The mean value and the standard deviation value for this figure are 1.83 dB and 6.60 dB respectively.

In Fig. 14, ray-tracing simulation is conducted for an empty pedestrian tunnel scenario, and plotted against the measurement results taken when the tunnel was empty (data from Fig. 7). Wooden sidewall (plywood) with a relative dielectric constant value of 2.1 is used for ray-tracing simulation [30]. As for the ceiling and ground, a relative dielectric constant value of 5 is used for normal strength concrete estimation [30]. The ray tracing program is written in MATLAB based on our experience in the development and implementation of ray tracing algorithms [31], [32]. The total rays considered in the ray-tracing simulation bouncing off the

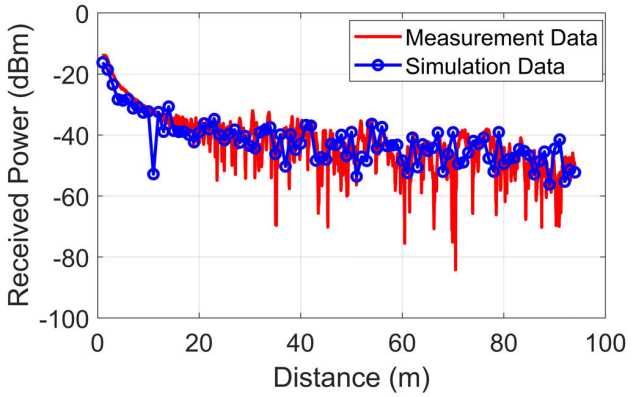

FIGURE 14. A comparison between ray-tracing simulation and measurement taken inside the empty pedestrian tunnel.

TABLE 2. Mean and standard deviation values.

	20m	50m	94m
Mean (dBm)	-40.8772	-51.3987	-55.3054
Standard Deviation (dBm)	2.9127	4.93067	5.78498

surrounding walls are the direct ray, ground reflected ray, top ceiling-reflected ray, and side walls-reflected rays (up to ten order of reflections). Where ground and ceiling are concerned, only the first order reflection is concerned. But for the side walls reflection, they can involve up to ten order reflections. Nevertheless, for the first 30 m along the measurement route, reflection from the side walls is not considered due to the dominant direct ray path. The mean value and the standard deviation value for Fig. 14 are 0.31dB and 7.23dB respectively.

V. FADE MARGIN ANALYSIS

Fade margin is a design allowance to ensure certain service reliability can be maintained through accommodating the expected deep fades in the wireless link. Assuming the received signal strength with shadow fading is log-normally distributed, applying curve fitting gives the following results for the mean and standard deviation at distances 20 m, 50 m, and 94 m respectively, refer to Fig. 15. In addition to the plotting, these results are also tabled in Table 2, whereby the average standard deviation is 4.54 dBm.

Subsequently, equations (2) – (4) are used to evaluate the Fade Margin (FM) for 90% SR [33], where σ_W is the standard deviation of received signal power in a given cell, and N is the path loss exponent. Using $\sigma_W = 4.54$ and $N = 1.40$, the FM for 90% SR is calculated to be about 5.82 dB. These values are useful for the prediction of the coverage range of small cell base station deployed in the pedestrian tunnel.

$$SR = \frac{1}{2}\left\{1 + erf\ (p) + \exp\left(\frac{1+2pq}{q^2}\right)\left[1 - erf\left(\frac{1+pq}{q}\right)\right]\right\} \tag{2}$$

where

$$p = \frac{FM}{\sqrt{2}\sigma_W} \tag{3}$$

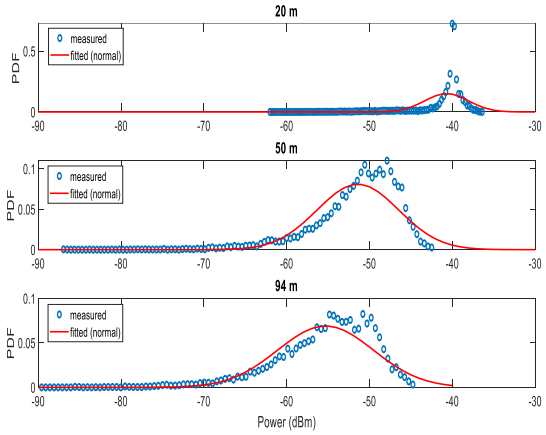

FIGURE 15. Probability density function (PDF) of the received power for crowded tunnel at 20, 50 and 94 m.

$$q = \frac{N \log_{10} e}{\sqrt{2}\sigma_W} \tag{4}$$

VI. CONCLUSION

In this project, we studied the propagation environment of a pedestrian tunnel in Kuala Lumpur at 24 GHz – an unlicensed band in Malaysia. Our findings suggest that pedestrian movements affect the signal very much at the millimeter wave bands. For one, in the presence of pedestrian, especially many and with frequent movement, the variation of the received signal strength is sharp and drastic. This is unlike a quiet empty tunnel scenario where relatively a much more consistent signal strength can be received. These two observations are valid not only for the measurement results, but they are consistent across the simulation results by means of ray-tracing technique. In the former, the case of a crowded pedestrian tunnel scenario, human scattering effects have been simulated. Whereas for the latter, the case of an empty pedestrian tunnel scenario, the bouncing of rays off the surrounding walls such as ceiling, floor, and the side walls are simulated. In both cases, the ray-tracing simulation results bear a close resemblance to the measurement results.

Where directional antennas such as horn antennas are used in the equipment set up, we found that the position of the Tx only matters for the first portion of the measurement route, e.g. for the first 15 m or so, after which no difference can be recorded when the separation distance between the Tx and Rx increases further. On the same note of directional antennas, we postulate to place the Tx antenna higher within the allowable range to ensure stronger received signal reception in the pedestrian tunnel. From the computed path loss exponent of the crowded tunnel (Fig. 10) at 1.40, and the computed standard deviation of the received signal power in a given cell at 4.54, the FM for 90% SR is calculated to be about 5.82 dB. The findings of this work have a wider application to other similar structure around the globe. They contribute towards ensuring wireless connectivity for the general users of the pedestrian tunnels anywhere in the world. Also, because horn antennas have been utilized in the measurement setup, we have emulated the actual beamforming technique whereby narrow beam antennas are used. Hence our results are applicable for massive MIMO implementation for 5G communications. For future work, other researchers may want to explore further on the optimal heights and positions of the transmitter in various shaped tunnels via simulations and measurements. They may also look into the size of the tunnel, the characteristics of the materials that were used to build the tunnel, as well as the depth of the tunnel, among others.

REFERENCES

[1] A. Emslie, R. Lagace, and P. Strong, "Theory of the propagation of UHF radio waves in coal mine tunnels," *IEEE Trans. Antennas Propag.*, vol. AP-23, no. 2, pp. 192–205, Mar. 1975.

[2] A. Hrovat, G. Kandus, and T. Javornik, "A survey of radio propagation modeling for tunnels," *IEEE Commun. Surveys Tuts.*, vol. 16, no. 2, pp. 658–669, 2nd Quart., 2014.

[3] K. Guan, Z. Zhong, J. I. Alonso, and C. Briso-Rodriguez, "Measurement of distributed antenna systems at 2.4 GHz in a realistic subway tunnel environment," *IEEE Trans. Veh. Technol.*, vol. 61, no. 2, pp. 834–837, Feb. 2012.

[4] Z. Sun and I. F. Akyildiz, "A mode-based approach for channel modeling in underground tunnels under the impact of vehicular traffic flow," *IEEE Trans. Wireless Commun.*, vol. 10, no. 10, pp. 3222–3231, Oct. 2011.

[5] H. Viittala, S. Soderi, J. Saloranta, M. Hamalainen, and J. Iinatti, "An experimental evaluation of WiFi-based vehicle-to-vehicle (V2V) communication in a tunnel," in *Proc. IEEE 77th Veh. Technol. Conf. (VTC Spring)*, Dresden, Germany, Jun. 2013, pp. 1–5.

[6] N. Prediger and A. Plattner, "Propagation measurements at 60 GHz in railroad tunnels," in *IEEE MTT-S Int. Microw. Symp. Dig.*, San Diego, CA, USA, 1994, pp. 1085–1087.

[7] G. Li, B. Ai, K. Guan, R. He, Z. Zhong, L. Tian, and J. Dou, "Path loss modeling and fading analysis for channels with various antenna setups in tunnels at 30 GHz band," in *Proc. 10th Eur. Conf. Antennas Propag. (EuCAP)*, Davos, Switzerland, Apr. 2016, pp. 1–5.

[8] X. Yin, X. Liu, G. Zheng, A. Saleem, and X. Zhai, "28-GHz channel characterization for a short tunnel," *IEEE Microw. Wireless Compon. Lett.*, vol. 28, no. 12, pp. 1146–1148, Dec. 2018.

[9] Y. Jiang, G. Zheng, X. Yin, A. Saleem, and B. Ai, "Performance study of millimetre-wave MIMO channel in subway tunnel using directional antennas," *IET Microw., Antennas Propag.*, vol. 12, no. 5, pp. 833–839, Apr. 2018.

[10] D. He, B. Ai, K Guan, Z. Zhong, B. Hui, J. Kim, H. Chung, and I. Kim, "Channel measurement, simulation, and analysis for high-speed railway communications in 5G millimeter-wave band," *IEEE Trans. Intell. Transp. Syst.*, vol. 19, no. 10, pp. 3144–3158, Oct. 2018.

[11] K. Guan, B. Ai, B. Peng, D. He, G. Li, J. Yang, Z. Zhong, and T. Kurner, "Towards realistic high-speed train channels at 5G millimeter-wave band—Part I: Paradigm, significance analysis, and scenario reconstruction," *IEEE Trans. Veh. Technol.*, vol. 67, no. 10, pp. 9112–9128, Oct. 2018.

[12] A. Hrovat, T. Javornik, and K. Guan, "Analysis of radio wave propagation at millimeter-wave band in tunnels for 5G communications," in *Proc. 22nd Int. Conf. Appl. Electromagn. Commun. (ICECOM)*, Dubrovnik, Croatia, Sep. 2016, pp. 1–5.

[13] A. Hrovat, K. Guan, and T. Javornik, "Traffic impact on radio wave propagation at millimeter-wave band in tunnels for 5G communications," in *Proc. 11st Eur. Conf. Antennas Propag. (EUCAP)*, Paris, France, Mar. 2017, pp. 2903–2906.

[14] M. Ghaddar, I. B. Mabrouk, M. Nedil, K. Hettak, and L. Talbi, "Deterministic modeling of 5G millimeter-wave communication in an underground mine tunnel," *IEEE Access*, vol. 7, pp. 116519–116528, 2019.

[15] R. Charbonnier, M. Z. Aslam, Y. Corre, and Y. Lostanlen, "Mixing deterministic and stochastic propagation for assessing mmWave small-cell networks," in *Proc. 11st Eur. Conf. Antennas Propag. (EUCAP)*, Paris, France, Mar. 2017, pp. 136–140.

[16] Y. Corre, R. Charbonnier, M. Z. Aslam, and Y. Lostanlen, "Assessing the performance of a 60-GHz dense small-cell network deployment from ray-based simulations," in *Proc. IEEE 21st Int. Workshop Comput. Aided Model. Design Commun. Links Netw. (CAMAD)*, Toronto, ON, Canada, Oct. 2016, pp. 213–218.
[17] S. Collonge, G. Zaharia, and G. E. Zein, "Influence of the human activity on wide-band characteristics of the 60 GHz indoor radio channel," *IEEE Trans. Wireless Commun.*, vol. 3, no. 6, pp. 2396–2406, Nov. 2004.
[18] F. Mokhtari-Koushyar, M. Alamdar, and M. Fakharzadeh, "Human body scattering modeling and measurement for millimeter-wave and 5G bands," in *Proc. IEEE Texas Symp. Wireless Microw. Circuits Syst. (WMCS)*, Mar. 2019, pp. 1–5.
[19] S. Ali and M. Junaid Mughal, "Narrowband characterization of the 60 GHz indoor radio channel in the presence of human bodies," in *Proc. 6th Int. Conf. Emerg. Technol. (ICET)*, Oct. 2010, pp. 226–229.
[20] C. M. Khoo and T. A. Ooi, "Key developments of tunnels in Malaysia," *Monthly Bull. Inst. Eng., Malaysia*, no. 7, pp. 13–20, Jul. 2018.
[21] W. H. Ting, T. A. Ooi, and B. K. Tan, "Tunneling activities in Malaysia," in *Proc. Southeast Asian Symp. Tunneling Underground Space Develop.*, Bangkok, Thailand, 1995, p. 1.
[22] *SMART Tunnel Listed Among CNN's Top 10 World's Greatest Tunnels*, Star Newspaper Malaysia, Petaling Jaya, Malaysia, Dec. 2016.
[23] *Stormwater Management and Road Tunnel (SMART)*. Accessed: Dec. 20, 2018. [Online]. Available: https://smarttunnel.com.my/
[24] S. Y. Lim, Z. Yun, and M. F. Iskander, "Propagation measurement and modeling for indoor stairwells at 2.4 and 5.8 GHz," *IEEE Trans. Antennas Propag.*, vol. 62, no. 9, pp. 4754–4761, Sep. 2014.
[25] S. Y. Lim, Z. Yun, and M. F. Iskander, "Modeling scattered EM field from a façade-like structure for wireless communications," in *Proc. IEEE Int. Symp. Antennas Propag. USNC/URSI Nat. Radio Sci. Meeting*, Spokane, WA, USA, Jul. 2011, p. 1.
[26] S. Y. Lim, A. K. Awelemdy, Z. Yun, and M. F. Iskander, "Experimental study of propagation characteristics in an open-trench drain," *IEEE Antennas Wireless Propag. Lett.*, vol. 15, pp. 60–63, 2016.
[27] Q. P. Soo, S. Y. Lim, D. W. G. Lim, K. M. Yap, and S. L. Lau, "Propagation measurement of a natural cave-turned-wine-cellar," *IEEE Antennas Wireless Propag. Lett.*, vol. 17, no. 5, pp. 743–746, May 2018.
[28] Q. P. Soo, S. Y. Lim, and D. W. G. Lim, "Investigation of rough surfaces for propagation modeling in caves," in *Proc. IEEE Int. Symp. Antennas Propag. USNC/URSI Nat. Radio Sci. Meeting*, Jul. 2018, pp. 555–556.
[29] S. Y. Lim, Z. Yun, and M. F. Iskander, "Radio propagation modeling: A unified view of the ray-tracing image method across emerging indoor and outdoor environments," in *The World of Applied Electromagnetics: In Appreciation of Magdy Fahmy Iskander*. Cham, Switzerland: Springer, 2018, pp. 301–328.
[30] H. L. Bertoni, *Radio Propagation for Modern Wireless Systems*. Upper Saddle River, NJ, USA: Prentice-Hall, 2000, pp. 15–39.
[31] M. F. Iskander and Z. Yun, "Propagation prediction models for wireless communication systems," *IEEE Trans. Microw. Theory Techn.*, vol. 50, no. 3, pp. 662–673, Mar. 2002.
[32] Z. Yun, Z. Zhang, and M. F. Iskander, "A ray-tracing method based on the triangular grid approach and application to propagation prediction in urban environments," *IEEE Trans. Antennas Propag.*, vol. 50, no. 5, pp. 750–758, May 2002.
[33] G.-Y. Liu, T.-Y. Chang, Y.-C. Chiang, P.-C. Lin, and J. Mar, "Path loss measurements of indoor LTE system for the Internet of Things," *Appl. Sci.*, vol. 7, no. 6, p. 537, May 2017.

QI PING SOO (Member, IEEE) received the M.Eng. degree (Hons.) in electrical and electronic engineering from the University of Nottingham Malaysia, in 2016, where he is currently pursuing the Ph.D. degree under the sponsorship of the Dean's scholarship, where he specializes in radio propagation modeling and prediction.

SOO YONG LIM (Senior Member, IEEE) received the B.Eng. degree (Hons.) in electronics majoring in telecommunications from Multimedia University, Malaysia, in 2003, and the Ph.D. degree in electrical engineering from the University of Hawaii at Manoa, USA, in 2010. She has been a Registered Professional Engineer with the Boards of Engineers Malaysia (BEM), since 2016. She is currently an Associate Professor with the Department of Electrical and Electronic Engineering, University of Nottingham Malaysia. Her current research interests include radio propagation modeling, channel measurements, and ray tracing.

She is a fellow of the Higher Education Academy (HEA), U.K. Since 2011, she has been started serving the IEEE Antennas and Propagation Society as a member of the Education Committee, and from 2015 forth, she commenced the role of an Associate Editor of the *Computer Applications in Engineering Education* (John Wiley & Sons). She remains in active service for both these roles hitherto. In July 2018, she was honored globally as the recipient of the IEEE AP-S Donald G. Dudley Jr. Undergraduate Teaching Award, with this citation "For modernizing the teaching of electromagnetics and for innovating its relevant curriculum design." Earlier in the same year in May 2018, she was selected worldwide as a Reviewer of the Month by IEEE Access, "for notable services and fine contributions towards the advancement of IEEE Access." This recognition is to thank her "for her valuable and thorough feedback on manuscript, and for her quick turnaround on reviews." Nationally within Malaysia, she received the 2020 IEEE Excellent Award, the 2019 IEEE Excellent Award, and also the 2018 IEEE Best Paper Award, all from the IEEE AP/MTT/EMC Awards Committee, Malaysia Chapter. In December 2017 and December 2018, she received the Research Award Certificate (Bronze) from the Faculty of Engineering, University of Nottingham Malaysia. In 2012, she won the Award for Achievement in Research for Early Career Researchers, Sunway University; and a bronze medal at the Malaysia Technology Expo, awarded by the Malaysian Association of Research Scientists.

NURHIDAYAH RUSLI received the M.Eng. degree (Hons.) in electrical and electronic engineering from the University of Nottingham Malaysia, in 2018.

KA HENG CHONG received the M.Eng. degree (Hons.) in electrical and electronic engineering from the University of Nottingham Malaysia, in 2018. He is currently organizing the administration of the AstraZeneca vaccines in the National COVID-19 Immunisation Programme with the World Trade Centre, Malaysia.

DAVID WEE GIN LIM (Senior Member, IEEE) received the Bachelor of Engineering degree (Hons.) in electrical and electronic engineering from University College London, in 1997, and the Ph.D. degree in telecommunications engineering from Australian National University, from 2000 to 2004, after spending a few years in the industry. He is currently an Associate Professor with the Department of Electrical and Electronic Engineering, University of Nottingham Malaysia. His research interest includes the umbrella of wireless communications.

HENG-SIONG LIM (Senior Member, IEEE) received the B.Eng. degree (Hons.) in electrical engineering from Universiti Teknologi Malaysia, Malaysia, in 1999, and the M.Eng.Sc. and Ph.D. degrees in wireless communications from Multimedia University, Malaysia, in 2002 and 2008, respectively. He is currently a Professor with the Faculty of Engineering and Technology, Multimedia University. His research interests include the areas of signal processing for wireless communications and advanced digital communication receivers design.

ZHENGQING YUN (Senior Member, IEEE) received the Ph.D. degree in electrical engineering from Chongqing University, Chongqing, China, in 1994. He was an Assistant Researcher with the Hawaii Center for Advanced Communications (HCAC), from 2002 to 2005, where he became an Assistant Professor, in 2006. He was involved in Postdoctoral work with the University of Utah and Southeast University, China, before he joined the University of Hawaii at Manoa (UH), Honolulu, HI, USA, where he is currently an Associate Professor with the Hawaii Center for Advanced Communications (HCAC), College of Engineering His current research interests include radio propagation in complex environments, such as urban, indoor, and mountainous areas. He served as the Technical Program Co-Chair of the IEEE Antenna and Propagation Society International Symposium, Honolulu, in 2007, and the Technical Program Chair of the IEEE International Conference on Wireless Information Technology and Systems, Honolulu, in 2010 and 2016, and Maui, HI, USA, in 2012. He was an Associate Editor of the IEEE TRANSACTIONS ON VEHICULAR TECHNOLOGY and the IEEE TRANSACTIONS ON ANTENNAS AND PROPAGATION. He is currently an Associate Editor of the IEEE ACCESS.

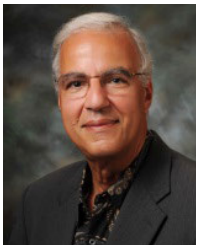

MAGDY F. ISKANDER (Life Fellow, IEEE) is currently the Director of the Hawaii Center for Advanced Communications (HCAC), and a Professor in electrical engineering with the College of Engineering, University of Hawaii at Manoa, Honolulu, HI, USA. He is also the Co-Director of the NSF Industry/University Cooperative Research Center with four other universities. He was the 2002 President of the IEEE Antennas and Propagation Society, a Distinguished Lecturer, and the Program Director with the Electrical, Communications, and Cyber Systems Division, National Science Foundation. He joined the University of Hawaii at Manoa, in 2002, and prior to that he was a Professor in electrical and computer engineering and an Engineering Clinic Endowed Chair Professor with the University of Utah. He has published over 270 papers in technical journals, holds nine patents, and has made numerous presentations at national/international conferences. He authored/edited several books, including the textbook *Electromagnetic Fields and Waves* (Prentice Hall, 1992, and Waveland Press, 2001; second edition 2012), and four books published by the Materials Research Society (MRS) on *Microwave Processing of Materials*. His research interests include computational and biomedical electromagnetics and wireless communications is funded by the National Science Foundation, National Institute of Health, Army Research Office, U.S. Army CERDEC, Office of Naval Research, and several corporate sponsors. He received many awards for excellence in research and teaching, including the University of Hawaii at Manoa Board of Regents' Medal for Excellence in Research, in 2013, the Board of Regents Medal for Teaching Excellence, in 2010, and the Hi Chang Chai Outstanding Teaching Award, in 2011 and 2014, which is based on votes by graduating seniors. He also received the IEEE MTT-S Distinguished Educator Award, in 2013, IEEE AP-S Chen-To Tai Distinguished Educator Award, in 2012, and Richard R. Stoddard Award from the IEEE EMC Society, in 1992. He received the Northrop Grumman Excellence in Teaching Award, in 2010, the American Society for Engineering Education (ASEE) Curtis W. McGraw National Research Award, in 1985, and, in 1991, the ASEE George Westinghouse National Award for Excellence in Education. Recently, his students won 1st place in the University of Hawaii at Manoa Business Plan Competition for the "CP Stethoscope" Project, and subsequently he founded the MiWa Technologies, LLC for medical devices and applications. He has been a Founding Editor of the *Computer Applications in Engineering Education* (CAE) journal (John Wiley & Sons), since 1992.